# **Establishing a Novel Qualitative Model to Predict Chemotherapy Response and Prognosis in Ovarian Cancer**

Junya Cao<sup>1,†</sup>, Xiaolin Luo<sup>1,†</sup>, Yi Ding<sup>1</sup>, Chanyuan Li<sup>2</sup>, Han Zhang<sup>1</sup>, Yanling Feng<sup>1,\*</sup>, Jihong Liu<sup>1,\*</sup>

Published: 1 May 2024

Background: Ovarian cancer is frequently associated with chemoresistance, which is the major cause of treatment failure. In this study, we utilized relative expression ordering (REO) of gene pairs to develop a novel model to predict chemotherapy response and prognosis in ovarian cancer. Moreover, we attempted to explore the mechanisms underlying ovarian cancer chemoresistance. Methods: Datasets were downloaded from publicly available databases, and differentially expressed gene pairs were filtered using Wilcoxon signed-rank test, Cox proportional hazards regression and Fisher's test to develop the model. Subsequently, the efficacy was validated by Kaplan–Meier analysis in training and validation sets. Comprehensive investigations were performed to investigate pathway variation, immune infiltration, and single-cell analysis. Next, gene expression was measured in chemoresistant ovarian cancer cells and their parent cells, and risk scores were calculated. Finally, a series of experiments were conducted to evaluate the regulatory impacts on chemosensitivity of lysyl oxidase-like 4 (LOXL4), one of the upregulated genes in chemoresistant cells.

Results: The developed model, comprising 19 genes for predicting chemoresistance and prognosis, demonstrated robust performance in training and five validation sets. Chemoresistant samples identified by this model exhibited enrichment of genes in four pathways and downregulation of genes in one pathway. Besides, chemoresistant samples displayed a lower abundance of various immune cell types, indicating immune suppression within the tumor microenvironment. Single-cell analysis indicated heterogeneity within samples, revealing cell populations that may survive after chemotherapy. Chemoresistant ovarian cells exhibited higher risk scores compared to their parent cells, and *LOXL4* was found to modulate cisplatin sensitivity in ovarian cancer cells. Conclusions: This study presents a novel prognostic model and provides possible therapeutic targets for further research in ovarian cancer.

Keywords: ovarian cancer; chemoresistance; prognostic model; LOXL4

# Introduction

Ovarian cancer represents a major global health challenge and ranks among the leading causes of cancer deaths in women worldwide. It is frequently diagnosed at advanced stages and is associated with poor prognosis [1,2]. The standard treatment approach for ovarian cancer is primary cytoreductive surgery, followed by platinum-based chemotherapy. About 20% of patients exhibit initial resistance to platinum-based regimens, and those who initially respond well to the treatment may develop acquired chemoresistance and experience recurrence eventually [3]. The development of chemoresistance poses a significant hurdle in the management of ovarian cancer, underscoring the critical need for identifying patients at risk of chemore-

sistance for prognosis stratification and tailored treatment strategies.

Chemoresistance in ovarian cancer can be attributed to a multitude of factors, such as reduced uptake and accelerated elimination of chemotherapeutic drugs, increased DNA repair, inhibition of apoptosis, metabolic remodeling of cancer cells, and interactions with the tumor microenvironment (TME) [4,5]. Genes involved in these pathways, such as *BRCA1/2*, *CCNE1* and *ABCB1*, were acknowledged as markers of responsiveness to chemotherapy. It has been discovered that dysfunction of more than one of these genes usually coincides with the development of chemoresistance [6]. Currently, various gene panels are available to predict chemotherapy response and prognosis in patients with ovarian cancer. Nevertheless, signatures based on quanti-

<sup>&</sup>lt;sup>1</sup>Department of Gynecologic Oncology, State Key Laboratory of Oncology in South China, Guangdong Provincial Clinical Research Center for Cancer, Sun Yat-Sen University Cancer Center, 510060 Guangzhou, Guangdong, China

<sup>&</sup>lt;sup>2</sup>Department of Gynecologic Oncology, Women's Hospital, Zhejiang University School of Medicine, 310006 Hangzhou, Zhejiang, China

<sup>\*</sup>Correspondence: fengyl@sysucc.org.cn (Yanling Feng); liujh@sysucc.org.cn (Jihong Liu)

<sup>&</sup>lt;sup>†</sup>These authors contributed equally.

tative transcriptional data often show low stability, which can be attributed to factors such as tumor cell proportion in samples, RNA degradation, amplification bias, batch effects, and cross-sample normalization method [7,8]. In contrast, within-sample relative expression ordering (REO) of genes, which represents qualitative characteristics of individual samples, is robust against these disturbances [9–11]. Consequently, REOs have been utilized in disease classification. Herein, we aimed to develop a prognostic model for ovarian cancer based on REOs in samples exhibiting disparate responses to chemotherapy. Furthermore, we investigated the biological features of patients with chemoresistant ovarian cancer and sought to identify biomarkers and potential therapeutic targets of platinum resistance.

#### Materials and Methods

# Data Acquisition and Preprocessing

Datasets used in this study were procured from the following publicly available databases: The Cancer Genome Atlas (TCGA), International Cancer Genome Consortium (ICGC), and Gene Expression Omnibus (GEO). Processed TCGA data were downloaded from Xena (http://xena.ucsc.edu/). The OV-AU dataset was retrieved from the ICGC data portal (https://dcc.icgc.org/). GSE102073, GSE26193, and GSE51088 were downloaded from GEO (https://www.ncbi.nlm.nih.gov/geo/).

The training set "GSE102073-response" was derived from GSE102073, which included 70 samples annotated with platinum response information. Validation datasets encompassed GSE102073 (all 84 samples), TCGA-OV, OV-AU, GSE26193, and GSE51088. Patient characteristics of datasets are shown in **Supplementary Tables 1,2**.

# Construction of REO-Based Prognostic Model

Samples within the training set were classified into two groups: chemoresistant (n = 11) or chemosensitive (n = 59) group. Chemoresistance was defined as relapse occurring within 6 months after completing primary chemotherapy, and chemosensitivity was defined as relapse occurring over 6 months after completing primary chemotherapy.

The model was developed as per the process described by Liu *et al.* [11] under R environment (Ver. 3.6.3, University of Auckland, Auckland, New Zealand). Differentially expressed genes (DEGs) between the groups were identified using Wilcoxon signed-rank test. Subsequently, univariate Cox proportional hazards regression test was employed to identify DEGs associated with prognosis. Fisher's test was then applied to assess whether the pattern of Gi > Gj or Gi < Gj (for a gene pair composed of two DEGs, Gi and Gj) occurred more frequently in chemoresistant samples than in chemosensitive ones. The final model comprised gene pairs identified through the aforementioned processes, and the risk score for each sample was increased by 1 if one of these gene pairs was present. R package

'pROC' (Ver. 1. 18. 0, https://xrobin.github.io/pROC/) was used to plot receiver operating characteristic (ROC) curve and determine optimal classification threshold for the model [12].

#### Verification of Prognostic Prediction Efficacy

The risk scores calculated for all samples in a dataset were stratified based on the established threshold to classify the samples into chemoresistant or chemosensitive group. Kaplan–Meier survival curves were generated and subjected to log-rank test to assess overall survival (OS) differences. In validation sets, if gene expression data in the model were missing, corresponding DEG pairs were not scored, but the threshold remained unchanged.

#### Gene Set Variation Analysis (GSVA)

Fifty 'Hallmark' gene sets covering the basic biological processes for human, obtained from the Molecular Signature Database (MSigDB, http://www.gsea-m sigdb.org/gsea/msigdb/index.jsp), were widely used in the gene set enrichment analysis [13]. employed these gene sets to investigate perturbations of pathways leading to chemoresistance. R packages 'GSVA' (Ver. 1.46.0, https://bioconductor.org/packages/ 3.16/bioc/html/GSVA.html) [14] and 'GSEABase' (Ver. 1.60.0, https://bioconductor.org/packages/3.16/bioc/html/ GSEABase.html) [15] were used to process expression data and perform gene set variation analysis (GSVA). R package 'ggplot2' (Ver. 3.4.2, https://ggplot2.tidyverse.org/) [16] was employed to draw boxplots for comparison of gene set enrichment between the groups.

# Immune Infiltration Analysis

Transcriptome-based immune cell infiltration data of TCGA samples were downloaded from xCell (https://xcel l.ucsf.edu/), including data calculated using the CIBER-SORT, EPIC, quanTIseq, TIMER, and xCell algorithms. These samples were categorized into chemoresistant or chemosensitive group, as previously described, and differences in immune cell infiltration between these groups were assessed using student's *t*-test.

#### Single-Cell Data Acquisition and Preprocessing

Single-cell expression matrices data and cell annotation information of the GSE154600 dataset were retrieved using TISCH (http://tisch.comp-genomics.org/). R package 'Seurat' (Ver. 4.1.1, https://satijalab.org/seurat/) [17] was used to process single-cell data, while 'ggplot2' was used for plotting. The cells were clustered using principal component analysis, followed by t-distributed stochastic neighbor embedding (t-SNE) dimension reduction. The cell populations were annotated based on the information file of TISCH. Expression for all genes in the panel was calculated and then visualized via a dot plot. Each single-



cell was scored and classified as being chemoresistant or chemosensitive based on the model, and two groups were presented for each cell cluster and each patient.

#### Cell Culture

The SKOV3 human ovarian cancer cell line utilized in this study was obtained from the China Academy of Medical Science (Beijing, China) and was authenticated prior to purchase. The COV504 and HEY human ovarian cancer cell lines were maintained at the Sun Yat-Sun University Cancer Center and were authenticated by the China Center for Type Culture Collection (Wuhan, China) (Supplementary File 2). Mycoplasma testing has been performed. The cells were cultured in Dulbecco's modified Eagle's medium (SH30243.01, Hyclone, Marlborough, MA, USA) supplemented with 10% fetal bovine serum (FSP500, ExCell Bio, Suzhou, China) in a humidified incubator at 37 °C with 5% CO<sub>2</sub>. Only cells that had been confirmed as mycoplasma-free were used in the subsequent experiments (Supplementary Fig. 1).

To establish cisplatin-resistant sublines, cells originating from SKOV3 and COV504 parent lines were subjected to increasing doses of cisplatin (601231004, Hansoh Pharma, Lianyungang, China), until they became accustomed to stable growth in medium supplemented with 2  $\mu$ M of cisplatin.

5′-**SiRNAs** (sil targeting sequence: GGTGCAATGTCCCTAACAT-3', si2 targeting sequence: 5'-CCGTGGAGGTGAAGTATGA-3') targeting oxidase-like 4 (LOXL4) were transfected into COV504 and HEY cells using Lipofectamine RNAiMAX Reagent (13778150, Thermo Fisher Scientific, Waltham, MA, USA) to induce LOXL4 knockdown in these cells. Scramble RNA served as negative control, and expression level of LOXL4 was verified to be equivalent in wild-type cell and scramble RNA-transfected cell (Supplementary Fig. 2). Both scramble RNA and siRNAs were synthesized by RiboBio company (Guangzhou, China).

## Cytotoxicity Assay

Cells were seeded in 96-well plates at a density of  $2 \times 10^3$  cells/well, and the media were replaced with different concentrations of cisplatin after 8 hours. After 72 hours of incubation, cytotoxicity assay was performed using Cell Counting Kit-8 (CK04, Dojindo, Kumamoto, Japan), as per manufacturer's instructions. The absorbance at 450 nm was measured by BioTek Synergy H1 (20033013, Agilent, Santa Clara, CA, USA). The half-maximal inhibitory concentration (IC $_{50}$ ) of cells was calculated using GraphPad Prism (Ver. 9.0.0, GraphPad Software, San Diego, CA, USA).

# Reverse-Transcription Real-Time Quantitative Polymerase Chain Reaction (RT-qPCR)

Total RNA was extracted using TRIzol (15596018, Thermo Fisher Scientific, Waltham, MA, USA), and complementary DNA was synthesized using PrimeScript<sup>TM</sup> RT Reagent Kit with gDNA Eraser (RR047A, Takara, Shiga, Japan). TB Green® Premix Ex Taq<sup>TM</sup> (RR420A, Takara, Shiga, Japan) was used in RT-qPCR, in adherence with manufacturer's instructions. Primer sequences are listed in **Supplementary Table 3**. Expression of genes was showed by quantity ratios of target genes to control gene *GAPDH*. Risk scores of cells were calculated as previously described in section Construction of REO-Based Prognostic Model.

## Western Blotting

Cells were lysed in RIPA lysis buffer (P0013B, Beyotime, Shanghai, China) containing 1 mM PMSF on ice. The protein products were separated by 7.5% SDS-PAGE and transferred onto polyvinylidene difluoride (PVDF) membranes according to standard procedures. The membranes were blocked with 5% non-fat milk in 0.05% Tween20/PBS, and then incubated with primary antibodies at 4 °C overnight. The antibody against LOXL4 (ab313797) was obtained from Abcam (Cambridge, UK), and the antibody against GAPDH (2118) was obtained from Cell Signaling Technology (Danvers, MA, USA). The dilution rate of anti-GAPDH and anti-LOXL4 is 1:1000. Protein bands were then incubated with an HRP-conjugated secondary antibody (1:5000, W4011/W4021, Promega, Madison, WI, USA). The signals were detected using ECL detection reagents (K-12045, advansta, San Jose, CA, USA) by ChemiDoc Touch (733BR3655, Biorad, Hercules, CA, USA).

#### Cell Apoptosis Assay

Cells were seeded into 6-well plates at a density of  $1.5 \times 10^5$  cells/well and incubated overnight. Then, medium with 2  $\mu$ M cisplatin or control medium was added to each well. After 48 hours, the cells were collected for apoptosis assay using Annexin V-FITC/PI Apoptosis Detection Kit (FXP018, 4A Biotech, Suzhou, China). Data were collected using CytoFLEX LX (AD11023, Beckman Coulter, Brea, CA, USA) and processed using FlowJo (Ver. 10.8.1, BD Life Science, Ashland, OR, USA). The Annexin V+/PI- and Annexin V+/PI+ populations were summed to obtain the total proportion of apoptotic cells.

#### Statistical Analysis

Experimental data were presented as mean  $\pm$  standard deviation. Significance between 2 groups was assessed by two-tailed student's *t*-test and two-way analysis of variance (ANOVA) using GraphPad Prism (Ver. 9.0.0, GraphPad Software, San Diego, CA, USA). p < 0.05 was considered statistically significant.

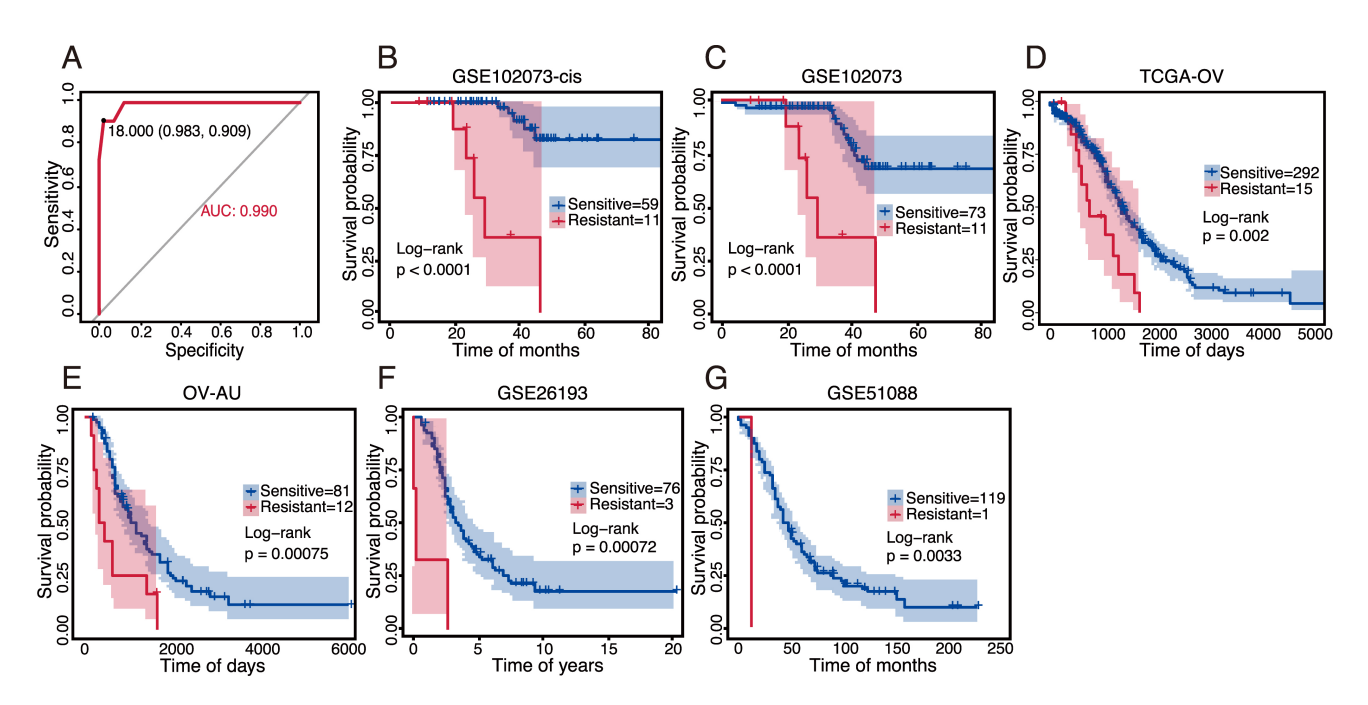


Fig. 1. Efficacy of the REO-based model for chemoresistance and prognosis prediction. (A) ROC curve of the model for the training set (GSE102073-response, n = 70). (B) Kaplan–Meier plot of OS for chemoresistant and chemosensitive samples in the training set. (C–G) Kaplan–Meier plots of OS for chemoresistant and chemosensitive samples in the validation sets: (C) GSE102073 (n = 84), (D) TCGA-OV (n = 307), (E) OV-AU (n = 93), (F) GSE26193 (n = 79), and (G) GSE51088 (n = 120). Abbreviations: ROC, receiver operating characteristic; OS, overall survival; TCGA, The Cancer Genome Atlas.

#### Results

## Chemotherapy-Related Prognostic Model for Ovarian Cancer Based on REO

The 70 samples in the training set were categorized into two groups based on their responses to platinum-based chemotherapy: chemoresistant (n = 11) or chemosensitive (n = 59) group. After conducting the Wilcoxon signedrank test, 141 DEGs were identified; these genes were subsequently filtered using the univariate Cox proportional hazards regression test, which resulted in 231 prognosisrelated gene pairs. Further screening was performed utilizing the Fisher's test to assess the stability of REO patterns within each group, yielding 29 gene pairs consisting of 19 genes, which were eventually integrated into a chemotherapy-related prognostic model (Table 1). All samples in the training set were assigned scores based on this model, resulting in a ROC curve with an area under the curve of 0.990. The threshold for classification was set at 18 (Fig. 1A).

# Efficacy of the REO-Based Model for Prognosis Prediction

Kaplan–Meier analysis showed that individuals classified as chemoresistant in the training set exhibited significantly poorer overall survival than those classified as chemosensitive (p < 0.0001) (Fig. 1B). This trend was consistently observed when testing five independent validation

datasets: GSE102073 (n = 84), TCGA-OV (n = 307), OV-AU (n = 93), GSE26193 (n = 79), and GSE51088 (n = 120) (Fig. 1C-G), indicating that the prognostic model performed well among datasets with regards to efficacy and robustness.

# Differential Pathway Enrichment in Chemoresistant and Chemosensitive Ovarian Cancer Samples

GSVA was employed to assess the enrichment of 50 hallmark gene sets from MSigDB database in samples from GSE102073-response dataset. Notably, the chemoresistant and chemosensitive groups exhibited different enrichment scores across gene pathways (Fig. 2A). Particularly, the chemoresistant group demonstrated significant enrichment of genes in the tumor necrosis factor- $\alpha$  (TNF- $\alpha$ ) signaling via nuclear factor-kappa B (NF- $\kappa$ B) pathway, hypoxia pathway, epithelial-mesenchymal transition (EMT) pathway, and coagulation pathway, while the chemosensitive group exhibited significant enrichment of genes in the E2F targets pathway (Fig. 2B).

# Suppression of Immune Cell Infiltration in Chemoresistant Ovarian Cancer Samples

Transcriptome-based immune cell information of TCGA samples was utilized to compare immune cell infiltration status between chemoresistant and chemosensitive groups using five distinct algorithms (Fig. 3). In summary, four, two, and nine distinct immune cell types exhib-

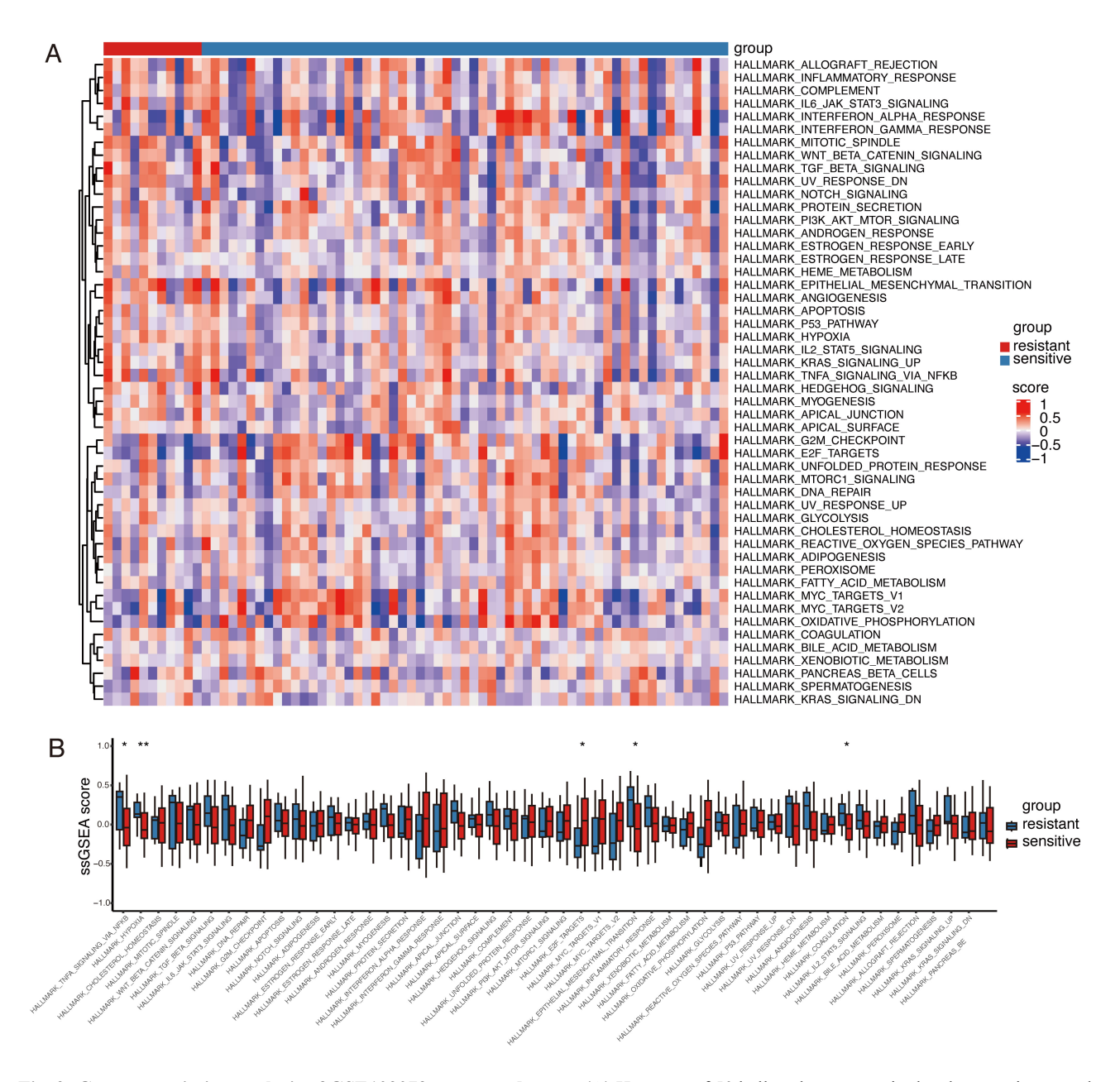


Fig. 2. Gene set variation analysis of GSE102073-response dataset. (A) Heatmap of 50 hallmark gene sets in the chemoresistant and chemosensitive groups. (B) Boxplots comparing gene set enrichment between the chemoresistant and chemosensitive groups. \*p < 0.05, \*\*p < 0.01.

ited significant differences between the groups when analyzed using CIBERSORT, quanTIseq, and xCell, respectively. In contrast, there were no significant differences in immune cells between the groups when assessed with EPIC and TIMER. Specifically, according to both CIBERSORT and xCell, CD4<sup>+</sup> memory T cell abundance was reduced in chemoresistant samples. Besides, chemoresistant samples showed a decrease in the abundance of natural killer (NK) cells according to xCell (NK cells) and CIBERSORT (resting NK cells). quanTIseq and EPIC exhibited the same tendency but without statistical significance. Furthermore, reductions in several other kinds of immune cell types in chemoresistant samples were identi-

fied, with only quanTIseq detecting an enrichment of uncharacterized cells. Collectively, these findings suggested the emergence of immune suppression in chemoresistant samples.

Chemotherapy Response Assessment Integrated with Single-Cell Analysis

GSE154600, encompassing five ovarian cancer samples with a total of 42,583 cells, was employed for single-cell analysis. Clustering of cells based on major-lineage annotation revealed distinct populations (Fig. 4A,B). Among the genes in our panel detected in this dataset, thioredoxin 2 (*TXN2*) displayed noticeable expression in various cell



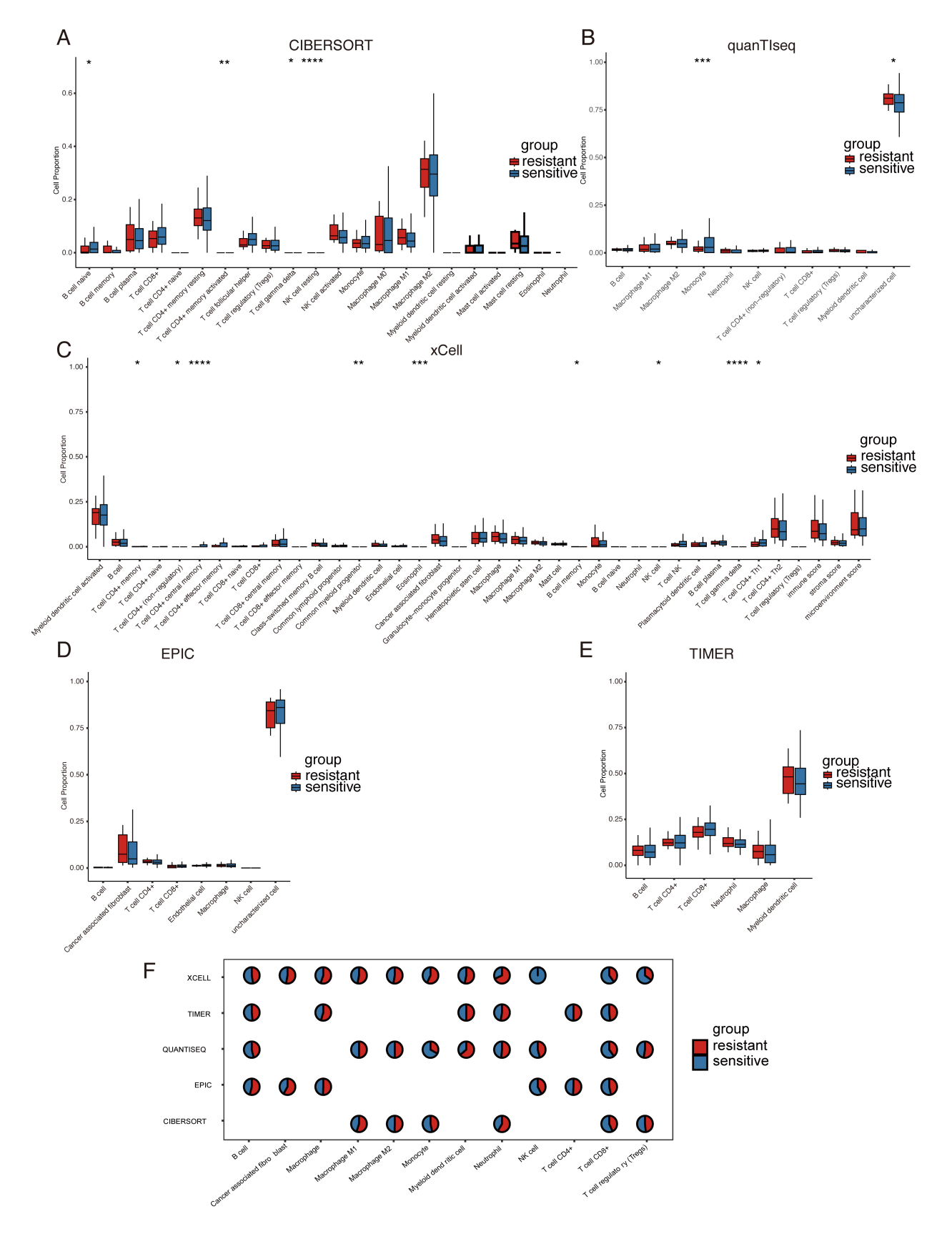


**Fig. 3.** Immune cell infiltration in chemoresistant and chemosensitive samples in TCGA-OV datasets. (A–E) Enrichment of immune cells in chemoresistant and chemosensitive samples based on CIBERSORT (A), quanTIseq (B), xCell (C), EPIC (D), and TIMER (E). (F) Summary of differences in immune cell infiltration between the groups. \*p < 0.05, \*\*p < 0.01, \*\*\*p < 0.001, \*\*\*\*p < 0.0001.

Table 1. REO-based gene pairs.

Gene1	Gene2	<i>p</i> -value	Resistant frequency	Sensitive_frequency	Туре
CDH18	ELFN2	0.00738	0.909091	0.457627	gene1>gene2
CDH18	GRID1	0.006806	0.818182	0.355932	gene1>gene2
CDH18	LRRN4	0.001005	0.818182	0.271186	gene1>gene2
CDH18	NAALADL2	0.006388	0.454545	0.084746	gene1>gene2
CDH18	NME6	$7.23 \times 10^{-6}$	0.727273	0.067797	gene1>gene2
CDH18	TXN2	0.000558	0.545455	0.067797	gene1>gene2
CDH18	ZNF441	$7.19\times10^{-5}$	0.636364	0.067797	gene1>gene2
CILP	DENND6A	$3.91\times10^{-5}$	1	0.338983	gene1>gene2
CILP	NAALADL2	0.001856	1	0.508475	gene1>gene2
CILP	SSBP2	0.000485	1	0.440678	gene1>gene2
CILP	TXN2	0.000485	1	0.440678	gene1>gene2
CILP	ZNF441	0.001856	1	0.508475	gene1>gene2
FGF18	NAALADL2	0.000163	0.636364	0.084746	gene1>gene2
FGF18	NME6	0.001827	0.636364	0.152542	gene1>gene2
FGF18	ZNF441	0.002911	0.636364	0.169492	gene1>gene2
LOXL4	NAALADL2	0.00124	0.727273	0.20339	gene1>gene2
LOXL4	NME6	0.000265	0.909091	0.305085	gene1>gene2
LOXL4	SSBP2	$7.19\times10^{-5}$	0.636364	0.067797	gene1>gene2
LOXL4	TXN2	$8.15\times10^{-5}$	0.727273	0.118644	gene1>gene2
LOXL4	ZNF441	0.000668	0.818182	0.254237	gene1>gene2
PMP22	SSBP2	0.001478	0.818182	0.288136	gene1>gene2
PMP22	TXN2	0.001613	0.909091	0.355932	gene1>gene2
PMP22	ZNF441	0.002243	1	0.525424	gene1>gene2
PTPRT	ZNF441	0.004518	0.363636	0.033898	gene1>gene2
C10orf55	FLG	0.002243	1	0.525424	gene1 <gene2< td=""></gene2<>
DENND6A	PMP22	0.001096	0.636364	0.135593	gene1 <gene2< td=""></gene2<>
FAM27E3	TEX26	0.00124	0.727273	0.20339	gene1 <gene2< td=""></gene2<>
NAALADL2	PMP22	$8.94\times10^{-5}$	1	0.372881	gene1 <gene2< td=""></gene2<>
NME6	PMP22	0.004788	1	0.542373	gene1 <gene2< td=""></gene2<>

Abbreviation: REO, relative expression ordering; *CDH18*, cadherin 18; *ELFN2*, extracellular leucine rich repeat and fibronectin type III domain containing 2; *GRID1*, glutamate ionotropic receptor delta type subunit 1; *LRRN4*, leucine rich repeat neuronal 4; *NAALADL2*, N-acetylated alpha-linked acidic dipeptidase like 2; *NME6*, NME/NM23 nucleoside diphosphate kinase 6; *TXN2*, thioredoxin 2; *ZNF441*, zinc finger protein 441; *CILP*, cartilage intermediate layer protein; *DENND6A*, DENN domain containing 6A; *SSBP2*, single stranded DNA binding protein 2; *FGF18*, fibroblast growth factor 18; *LOXL4*, lysyl oxidase-like 4; *PMP22*, peripheral myelin protein 22; *PTPRT*, protein tyrosine phosphatase receptor type T; *C10orf*55, chromosome 10 putative open reading frame 55; *FLG*, filaggrin; *FAM27E3*, family with sequence similarity 27 member E3; *TEX26*, testis expressed 26.

populations, particularly malignant cells, whereas peripheral myelin protein 22 (*PMP22*) expression was mainly detected in fibroblasts (Fig. 4C). Utilizing this panel, we classified 4178 cells as chemoresistant and the remaining as chemosensitive. Interestingly, chemoresistant cells were not only in malignant populations but also in other clusters, notably fibroblasts (Fig. 4D). Among the five patient-derived samples in the cohort, both chemoresistant and chemosensitive cells were identified in all samples. In particular, T61 and T90 exhibited the highest proportion of chemoresistant and chemosensitive cells, respectively (Fig. 4E).

LOXL4 was Overexpressed in Chemoresistant Ovarian Cancer Cells and Regulated Sensitivity to Cisplatin

The ovarian cancer cell lines SKOV3 and COV504 were exposed to low-concentration cisplatin to generate cisplatin-resistant cell lines, namely SKOV3-cis and COV504-cis, respectively, which were characterized by significantly elevated IC<sub>50</sub> to cisplatin (Fig. 5A). Expression of the 19 genes in our panel was then assessed in these cells by RT-qPCR, and risk scores were calculated. SKOV3-cis and COV504-cis cells exhibited higher risk scores than their corresponding parent cells, although these scores did not exceed the threshold of 18 (Fig. 5B). Notably,

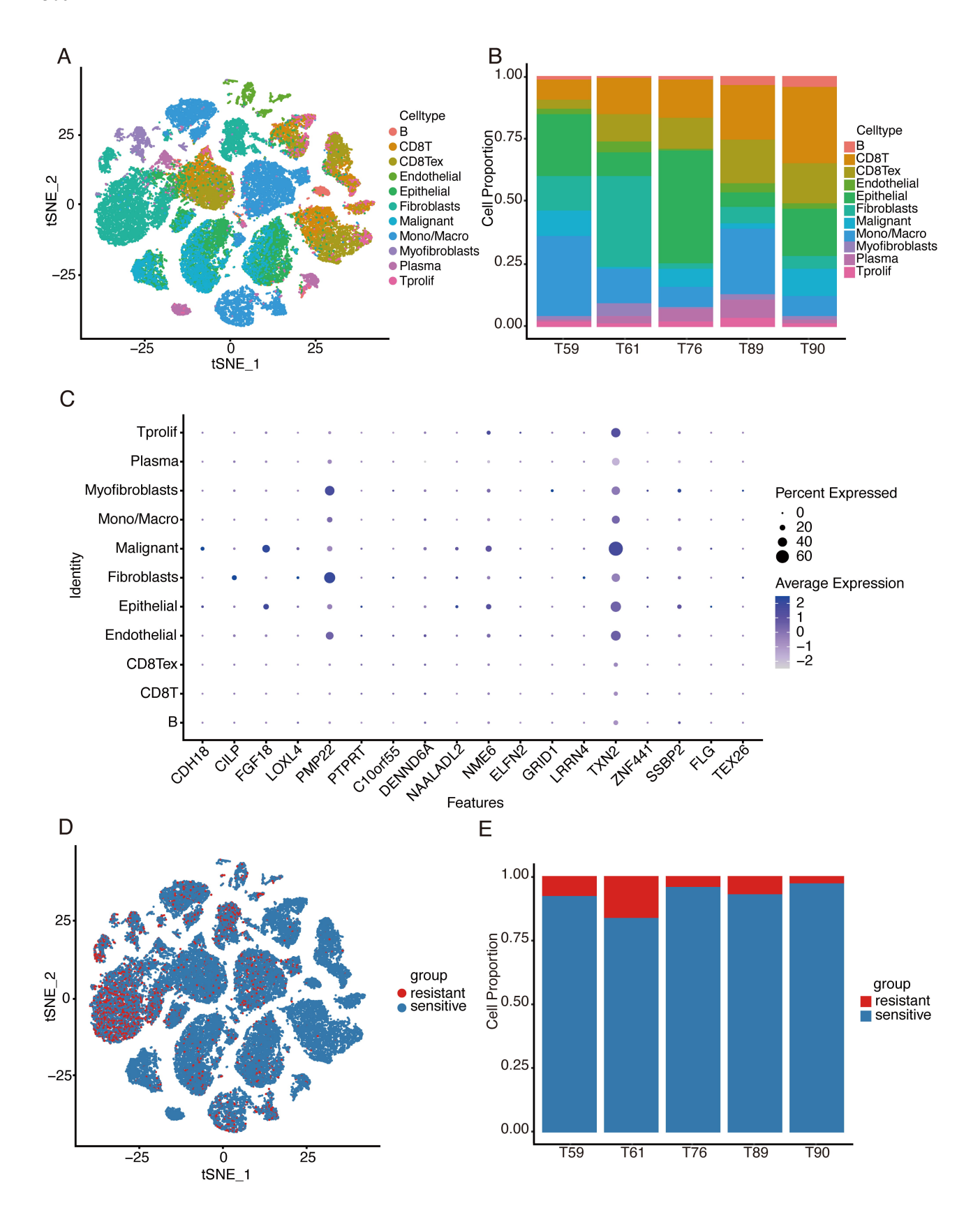


**Fig. 4.** Chemotherapy response assessment at single-cell level. (A) Visualization of cell clusters in GSE154600 using t-SNE. (B) Visualization of cell clusters in each patient in GSE154600. (C) Dot plot showing the expression pattern of genes in single-cell clusters. (D) Visualization of chemoresistant and chemosensitive cells in single-cell clusters. (E) Composition of chemoresistant and chemosensitive cells in each patient in GSE154600. Abbreviation: t-SNE, t-distributed stochastic neighbor embedding.

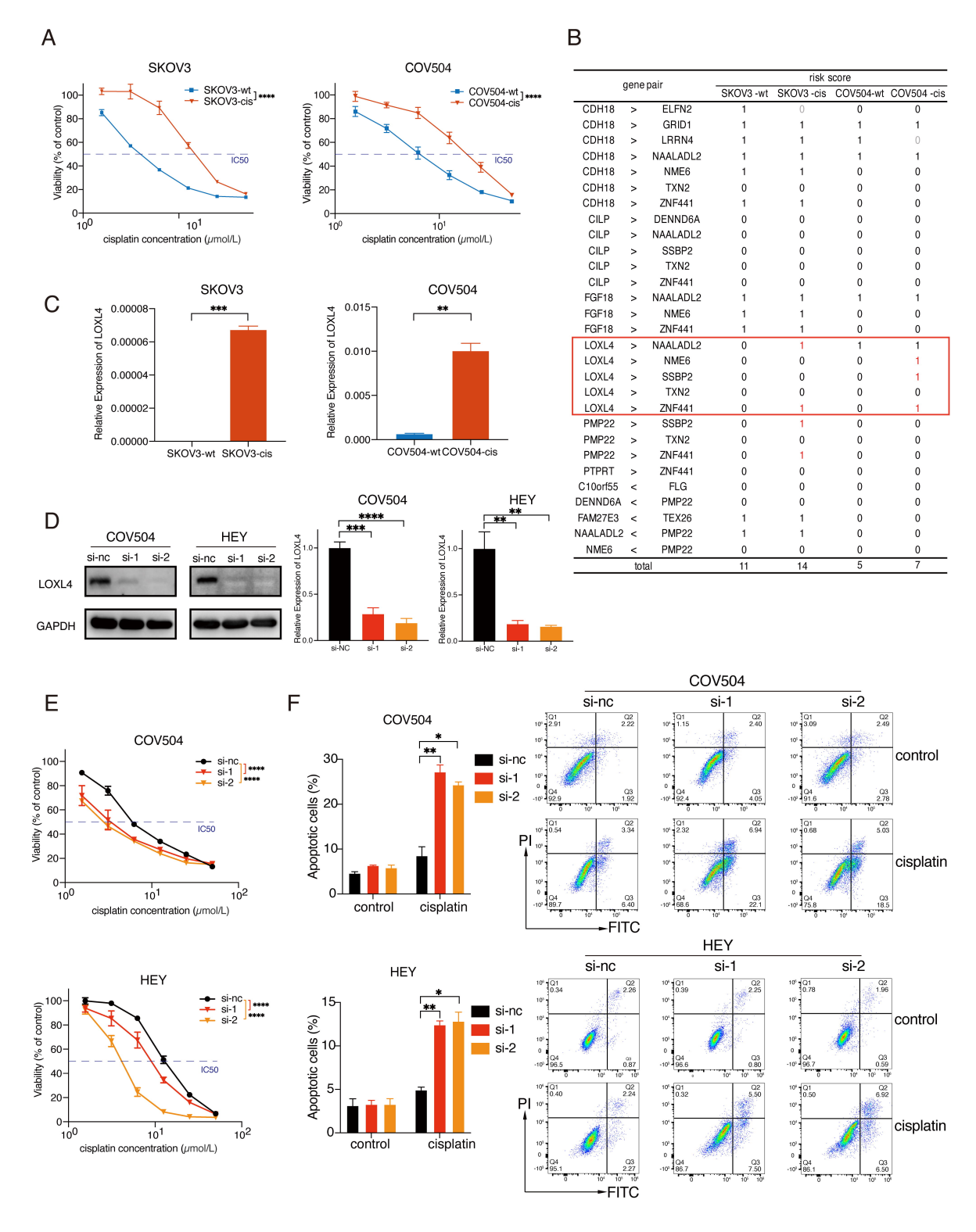


Fig. 5. LOXL4 was overexpressed in chemoresistant ovarian cancer cells and regulated sensitivity to cisplatin. (A) Cytotoxicity assay (Cell Counting Kit-8) in chemoresistant and wild-type ovarian cancer cell lines. (B) Risk scores of chemoresistant and wild-type ovarian cancer cell lines. Gene pairs containing LOXL4 were marked by the red box. (C) LOXL4 expression levels of ovarian cancer cells by RT-qPCR. (D) Knockdown of LOXL4 in ovarian cancer cells. (E) Cytotoxicity assay in LOXL4 knocked-down cells and negative control. (F) Cell apoptosis assay in LOXL4 knocked-down cells and negative control. \*p < 0.05, \*\*p < 0.01, \*\*\*\*p < 0.001, \*\*\*\*p < 0.0001. Abbreviations: IC50, half-maximal inhibitory concentration; RT-qPCR, reverse-transcription real-time quantitative polymerase chain reaction.

LOXL4 was significantly upregulated in both SKOV3-cis and COV504-cis cells as compared to that in wild-type cells, and gene pairs containing LOXL4 obviously contributed to the increase in risk scores, indicating a potential role of LOXL4 in cisplatin resistance of ovarian cancer cells (Fig. 5B,C).

We then generated ovarian cancer cell lines with LOXL4 knockdown using siRNAs (Fig. 5D). Knockdown of LOXL4 enhanced sensitivity to cisplatin in COV504 and HEY ovarian cells, as demonstrated by reduced IC $_{50}$  and an increased rate of cisplatin-induced apoptosis (Fig. 5E,F). Further studies are needed to investigate the mechanism of cisplatin resistance induced by LOXL4 in ovarian cancer.

#### Discussion

Ovarian cancer is the most lethal gynecological malignancy and is associated with late-stage diagnoses and high recurrence rates. In the present study, we built an REO-based prognostic model using transcriptome signatures for samples with disparate responses to chemotherapy. The model demonstarted robust efficacy in our training and validation sets. However, considering the relatively small sample size in this study, further validation in clinical practice is necessary.

Regulation of chemosensitivity is quite complex. Here, we utilized transcriptomic data to perform comprehensive analyses to unravel the underlying mechanism of chemoresistance in ovarian cancer. As per the findings of GSVA, genes associated with chemoresistant samples were enriched in TNF- $\alpha$  signaling via NF- $\kappa$ B pathway, hypoxia pathway, EMT pathway, and coagulation pathway, while those associated with chemosensitive samples were enriched in E2F targets pathway. The activation of the NF- $\kappa$ B pathway has been confirmed to contribute to chemoresistance and decreased survival in ovarian cancer [18-20]. Hypoxia, a typical characteristic of almost all solid tumors, has also been found to reduce responsiveness to cisplatin, paclitaxel, and 5-FU in ovarian cancer cells in previous studies [21–23]. The role of EMT, the E2F targets and coagulation pathway in chemoresistance remains controversial. Several studies have suggested that ovarian cancer with an epithelial signature is associated with better overall and disease-free survival [24]; however, as reported in several in vitro analyses [24,25], ovarian cancer with a mesenchymal signature shows preferential sensitivity to cisplatin. Previous research has shown that the E2F targets pathway activation is associated with favorable chemotherapy responses in prostate [26], colon [27], and triple-negative breast cancers [28], but it leads to poor prognosis in ER<sup>+</sup>/HER2<sup>-</sup> breast cancer [29]. A proteogenomic analysis conducted in ovarian cancer has indicated significantly lower expression of E2F transcription factors in refractory tumors as compared to that in sensitive tumors, which aligns with our results [30]. Relatively fewer studies

have hinted at a role of the coagulation pathway in therapy resistance. Mousset *et al.* [31] found that chemotherapy induces neutrophil extracellular trap formation, promoting chemoresistance of breast cancer lung metastases in mice. In addition, Jeon *et al.* [32] found that coagulation factor III is induced in senescence-associated glioblastoma cells in response to radiation, aiding cell evasion of therapeutic pressure. In light of the current set of findings, additional research is needed to confirm the role of these three pathways in ovarian cancer chemoresistance.

The immune suppression network, which attenuates antitumor immunity, is a primary driver of disease progression and treatment failure. The activity of immune effector cells, including CD4<sup>+</sup> T, CD8<sup>+</sup> T, and NK cells, is inhibited by not only tumor cells directly but also immunosuppressive T regulatory cells, immature dendritic cells, myeloid-derived suppressor cells, and tumor-associated macrophages [5,33]. Previous researches have indicated that immune cell infiltration status has a potential prognostic value for various cancers, such as gastric cancer and lung adenocarcinoma [34,35]. In this study, we found that chemoresistant ovarian cancer samples exhibited significantly lower infiltration of NK cells and certain CD4<sup>+</sup> T cell types, but not T regulatory cells, in comparison to chemosensitive ovarian cancer samples. This suggests that chemoresistant ovarian cancer shows a suppressed immune status, which aligns with the findings by Verma et al. [36] on breast cancer. Colletively, these findings suggest that the interaction of immune cells within the TME impacts treatment outcomes in patients with ovarian cancer, although the underlying mechanism warrants further investigation.

Single-cell sequencing is a powerful approach for investigating tumor composition and elucidating cellular heterogeneity. Our analysis at single-cell level revealed the composition of cells exhibiting different chemotherapy responses within each cluster and patient. Chemoresistant and chemosensitive ovarian cancer cells were found to coexist in every sample, albeit in varying proportions, indicative of heterogeneity within cancer tissues. It is reasonable to speculate that chemoresistant cells are able to partially survive chemotherapy, potentially causing recurrence eventually. While this dataset lacks survival information, it would be intriguing to explore whether chemoresistant cell percentage correlates with recurrence and poor prognosis. Notably, fibroblasts, in addition to malignant cells, were identified as chemoresistant cells, indicating the potential role of genes expressed among fibroblasts in resistance to chemotherapeutic agents.

When applying our model to ovarian cancer cell lines to evaluate their chemoresistant status, we found that cisplatin-resistant cells had higher risk scores than their parent cells, though these scores did not reach the threshold. This discrepancy may be due to some genes being expressed in cells within the TME rather than in tumor cells, as evident from the single-cell analysis. Among the individual genes



in our panel, we found that the upregulation of LOXL4 led to an increase in the risk scores of two cisplatin-resistant ovarian cancer cell lines. LOXL4, as a member of the LOX family, mediates collagen and elastin crosslinking in the extracellular matrix [37]. According to previous studies, LOXL4 serves as an oncogene in breast cancer [37], hepatocellular carcinoma [38], and gastric cancer [39]. However, in bladder cancer, LOXL4 repression reportedly induces multidrug resistance [40]. Besides, LOXL4 splice variants have been found to exert a positive effect on the metastatic potential of ovarian cancer cells [41]. The current study identified for the first time that knockdown of LOXL4 enhanced cisplatin sensitivity of ovarian cancer cells, as demonstrated by both cell toxicity and cell apoptosis assays, making contradictory findings compared to the analysis on bladder cancer as reported by Deng et al. [40]. Thus, further studies are warranted to elucidate the role of LOXL4 in ovarian cancer chemoresistance.

#### Conclusions

In conclusion, we developed a novel model for predicting chemotherapy response and prognosis with robust performance. Chemoresistant samples, as defined by our model, exhibit aberrant activation of pathways and decreased immune cell infiltration. At the single-cell level, we identified heterogeneity within ovarian cancer samples and the possible existence of residual populations surviving chemotherapy. We believe that *LOXL4*, as a prognostic marker and potential therapeutic target, is worthy of further research. Taken together, our findings provide insights into prognosis stratification and mechanisms underlying ovarian cancer chemoresistance.

# Availability of Data and Materials

The datasets generated during and analysed during the current study are available from the corresponding authors on reasonable request.

#### **Author Contributions**

The project was conceived and designed by JL, YF and JC. Data collection and analysis were performed by JC and XL. Experiments were performed by JC, YD and HZ. Figures and tables were organized by XL and CL. The manuscript was written by JC and YF, and revised by JL. The whole project was supervised by JL. All authors have been involved in revising it critically for important intellectual content. All authors gave final approval of the version to be published. All authors have participated sufficiently in the work to take public responsibility for appropriate portions of the content and agreed to be accountable for all aspects of the work in ensuring that questions related to its accuracy or integrity.

## Ethics Approval and Consent to Participate

Not applicable.

# Acknowledgment

Not applicable.

# **Funding**

This work was supported by the National Natural Science Foundation of China (No. 82272698 to JL, No.82102732 to XL).

#### Conflict of Interest

The authors declare no conflict of interest.

# Supplementary Material

Supplementary material associated with this article can be found, in the online version, at https://doi.org/10.23812/j.biol.regul.homeost.agents.20243805.341.

#### References

- [1] Siegel RL, Miller KD, Wagle NS, Jemal A. Cancer statistics, 2023. CA: a Cancer Journal for Clinicians. 2023; 73: 17–48.
- [2] Torre LA, Trabert B, DeSantis CE, Miller KD, Samimi G, Runowicz CD, et al. Ovarian cancer statistics, 2018. CA: a Cancer Journal for Clinicians. 2018; 68: 284–296.
- [3] Monk BJ, Herzog TJ, Tewari KS. Evolution of Chemosensitivity and Resistance Assays as Predictors of Clinical Outcomes in Epithelial Ovarian Cancer Patients. Current Pharmaceutical Design. 2016; 22: 4717–4728.
- [4] Yang L, Xie HJ, Li YY, Wang X, Liu XX, Mai J. Molecular mechanisms of platinum based chemotherapy resistance in ovarian cancer (Review). Oncology Reports. 2022; 47: 82.
- [5] Ghoneum A, Almousa S, Warren B, Abdulfattah AY, Shu J, Abouelfadl H, et al. Exploring the clinical value of tumor microenvironment in platinum-resistant ovarian cancer. Seminars in Cancer Biology. 2021; 77: 83–98.
- [6] Patch AM, Christie EL, Etemadmoghadam D, Garsed DW, George J, Fereday S, et al. Whole-genome characterization of chemoresistant ovarian cancer. Nature. 2015; 521: 489–494.
- [7] Patil P, Bachant-Winner PO, Haibe-Kains B, Leek JT. Test set bias affects reproducibility of gene signatures. Bioinformatics (Oxford, England). 2015; 31: 2318–2323.
- [8] Guan Q, Yan H, Chen Y, Zheng B, Cai H, He J, et al. Quantitative or qualitative transcriptional diagnostic signatures? A case study for colorectal cancer. BMC Genomics. 2018; 19: 99.
- [9] Liu H, Li Y, He J, Guan Q, Chen R, Yan H, et al. Robust transcriptional signatures for low-input RNA samples based on relative expression orderings. BMC Genomics. 2017; 18: 913.
- [10] Ao L, Guo Y, Song X, Guan Q, Zheng W, Zhang J, et al. Evaluating hepatocellular carcinoma cell lines for tumour samples using within-sample relative expression orderings of genes. Liver International: Official Journal of the International Association for the Study of the Liver. 2017; 37: 1688–1696.
- [11] Liu K, Geng Y, Wang L, Xu H, Zou M, Li Y, et al. Systematic exploration of the underlying mechanism of gemcitabine resistance in pancreatic adenocarcinoma. Molecular Oncology. 2022; 16: 3034–3051.

- [12] Robin X, Turck N, Hainard A, Tiberti N, Lisacek F, Sanchez JC, et al. pROC: an open-source package for R and S+ to analyze and compare ROC curves. BMC Bioinformatics. 2011; 12: 77.
- [13] Liberzon A, Birger C, Thorvaldsdóttir H, Ghandi M, Mesirov JP, Tamayo P. The Molecular Signatures Database (MSigDB) hallmark gene set collection. Cell Systems. 2015; 1: 417–425.
- [14] Hänzelmann S, Castelo R, Guinney J. GSVA: gene set variation analysis for microarray and RNA-seq data. BMC Bioinformatics. 2013; 14: 7.
- [15] Bioconductor. GSEABase: Gene set enrichment data structures and methods. 2023. Available at: https://bioconductor.org/pac kages/3.16/bioc/html/GSEABase.html (Accessed: 22 February 2024).
- [16] Wickham H. ggplot2: Elegant Graphics for Data Analysis. Springer-Verlag New York: New York, USA. 2016.
- [17] Hao Y, Hao S, Andersen-Nissen E, Mauck WM, 3rd, Zheng S, Butler A, et al. Integrated analysis of multimodal single-cell data. Cell. 2021; 184: 3573–3587.e29.
- [18] Devanaboyina M, Kaur J, Whiteley E, Lin L, Einloth K, Morand S, *et al.* NF-κB Signaling in Tumor Pathways Focusing on Breast and Ovarian Cancer. Oncology Reviews. 2022; 16: 10568.
- [19] Özeş AR, Miller DF, Özeş ON, Fang F, Liu Y, Matei D, et al. NF-κB-HOTAIR axis links DNA damage response, chemoresistance and cellular senescence in ovarian cancer. Oncogene. 2016; 35: 5350–5361.
- [20] Li F, Sethi G. Targeting transcription factor NF-kappaB to overcome chemoresistance and radioresistance in cancer therapy. Biochimica et Biophysica Acta. 2010; 1805: 167–180.
- [21] Dorayappan KDP, Wanner R, Wallbillich JJ, Saini U, Zingarelli R, Suarez AA, *et al.* Hypoxia-induced exosomes contribute to a more aggressive and chemoresistant ovarian cancer phenotype: a novel mechanism linking STAT3/Rab proteins. Oncogene. 2018; 37: 3806–3821.
- [22] Qin J, Liu Y, Lu Y, Liu M, Li M, Li J, *et al.* Hypoxia-inducible factor 1 alpha promotes cancer stem cells-like properties in human ovarian cancer cells by upregulating SIRT1 expression. Scientific Reports. 2017; 7: 10592.
- [23] Feng L, Shen F, Zhou J, Li Y, Jiang R, Chen Y. Hypoxia-induced up-regulation of miR-27a promotes paclitaxel resistance in ovarian cancer. Bioscience Reports. 2020; 40: BSR20192457.
- [24] Tan TZ, Miow QH, Miki Y, Noda T, Mori S, Huang RYJ, *et al.* Epithelial-mesenchymal transition spectrum quantification and its efficacy in deciphering survival and drug responses of cancer patients. EMBO Molecular Medicine. 2014; 6: 1279–1293.
- [25] Miow QH, Tan TZ, Ye J, Lau JA, Yokomizo T, Thiery JP, et al. Epithelial-mesenchymal status renders differential responses to cisplatin in ovarian cancer. Oncogene. 2015; 34: 1899–1907.
- [26] Kallenbach J, Atri Roozbahani G, Heidari Horestani M, Baniah-mad A. Distinct mechanisms mediating therapy-induced cellular senescence in prostate cancer. Cell & Bioscience. 2022; 12: 200.
- [27] Liu KP, Luo F, Xie SM, Tang LJ, Chen MX, Wu XF, et al. Glycogen Synthase Kinase 3β Inhibitor (2'Z,3'E)-6-Bromo-indirubin- 3'-Oxime Enhances Drug Resistance to 5-Fluorouracil Chemotherapy in Colon Cancer Cells. Chinese Journal of Cancer Research. 2012; 24: 116–123.
- [28] Anurag M, Jaehnig EJ, Krug K, Lei JT, Bergstrom EJ, Kim BJ, et al. Proteogenomic Markers of Chemotherapy Resistance and

- Response in Triple-Negative Breast Cancer. Cancer Discovery. 2022; 12: 2586–2605.
- [29] Oshi M, Takahashi H, Tokumaru Y, Yan L, Rashid OM, Nagahashi M, et al. The E2F Pathway Score as a Predictive Biomarker of Response to Neoadjuvant Therapy in ER+/HER2- Breast Cancer. Cells. 2020; 9: 1643.
- [30] Chowdhury S, Kennedy JJ, Ivey RG, Murillo OD, Hosseini N, Song X, *et al.* Proteogenomic analysis of chemo-refractory highgrade serous ovarian cancer. Cell. 2023; 186: 3476–3498.e35.
- [31] Mousset A, Lecorgne E, Bourget I, Lopez P, Jenovai K, Cherfils-Vicini J, *et al*. Neutrophil extracellular traps formed during chemotherapy confer treatment resistance via TGF-β activation. Cancer Cell. 2023; 41: 757–775.e10.
- [32] Jeon HM, Kim JY, Cho HJ, Lee WJ, Nguyen D, Kim SS, et al. Tissue factor is a critical regulator of radiation therapy-induced glioblastoma remodeling. Cancer Cell. 2023; 41: 1480–1497.e9.
- [33] Worzfeld T, Pogge von Strandmann E, Huber M, Adhikary T, Wagner U, Reinartz S, et al. The Unique Molecular and Cellular Microenvironment of Ovarian Cancer. Frontiers in Oncology. 2017; 7: 24.
- [34] Ning ZK, Hu CG, Huang C, Liu J, Zhou TC, Zong Z. Molecular Subtypes and CD4<sup>+</sup> Memory T Cell-Based Signature Associated With Clinical Outcomes in Gastric Cancer. Frontiers in Oncology. 2021; 10: 626912.
- [35] Choi H, Na KJ. Integrative analysis of imaging and transcriptomic data of the immune landscape associated with tumor metabolism in lung adenocarcinoma: Clinical and prognostic implications. Theranostics. 2018; 8: 1956–1965.
- [36] Verma C, Kaewkangsadan V, Eremin JM, Cowley GP, Ilyas M, El-Sheemy MA, et al. Natural killer (NK) cell profiles in blood and tumour in women with large and locally advanced breast cancer (LLABC) and their contribution to a pathological complete response (PCR) in the tumour following neoadjuvant chemotherapy (NAC): differential restoration of blood profiles by NAC and surgery. Journal of Translational Medicine. 2015; 13: 180.
- [37] Yin H, Wang Y, Wu Y, Zhang X, Zhang X, Liu J, et al. EZH2-mediated Epigenetic Silencing of miR-29/miR-30 targets LOXL4 and contributes to Tumorigenesis, Metastasis, and Immune Microenvironment Remodeling in Breast Cancer. Theranostics. 2020; 10: 8494–8512.
- [38] Li R, Wang Y, Zhang X, Feng M, Ma J, Li J, *et al.* Exosome-mediated secretion of LOXL4 promotes hepatocellular carcinoma cell invasion and metastasis. Molecular Cancer. 2019; 18:
- [39] Li RK, Zhao WY, Fang F, Zhuang C, Zhang XX, Yang XM, et al. Lysyl oxidase-like 4 (LOXL4) promotes proliferation and metastasis of gastric cancer via FAK/Src pathway. Journal of Cancer Research and Clinical Oncology. 2015; 141: 269–281.
- [40] Deng H, Lv L, Li Y, Zhang C, Meng F, Pu Y, et al. miR-193a-3p regulates the multi-drug resistance of bladder cancer by targeting the LOXL4 gene and the oxidative stress pathway. Molecular Cancer. 2014; 13: 234.
- [41] Sebban S, Golan-Gerstl R, Karni R, Vaksman O, Davidson B, Reich R. Alternatively spliced lysyl oxidase-like 4 isoforms have a pro-metastatic role in cancer. Clinical & Experimental Metastasis. 2013; 30: 103–117.